Journal of Umm Al-Qura University for Engineering and Architecture

journal homepage: https://uqu.edu.sa/en/jea

A New Virtual Synchronous Machine Control Structure for Voltage Source Converter in High Voltage Direct Current Applications

Hasan Alrajhi Alsiraji [a,*].

Department of Electrical Engineering, Umm al-Qura University, Makkah, Saudi Arabia.

ARTICLE INFO

Article History:
Submission date: 30 /9/2019
Accepted date: 18/12/2019

Keywords:
Inverters; Microgrid; Inertia emulation; Virtual Synchronous machine; Hybrid virtual synchronous machine

ABSTRACT

The high potential of integrating renewable energy resources into the power system using voltage source converters (VSCs) raises some system stability issues due to the absence of inertia in VSCs. The virtual synchronous machine (VSM) control concept is consequently introduced to mimic the properties of traditional synchronous machines. Several VSM control algorithms with different structures have been introduced in literature. However, since all VSM controllers are co-linked as an active and reactive power control, it is difficult to achieve a unity power factor from a VSC-based VSM, a feature which is more likely favoured in a multi-terminal HVDC systems. This paper proposes a new way to implement the VSM control concept which offers several advantages. The proposed hybrid virtual synchronous machine (HVSM) provides a fully decoupled independent active and reactive power control. This paper further presents a comparative comprehensive study of the proposed HVSM with the existing VSM in literature. The system has been validated and investigated in a time-domain simulation environment, namely PSCAD/EMTDC. The simulation results show significant results that will further extend the field of virtual synchronous machine research.

1. Introduction

In the light of the growing global demand for electrical power, there is a strong need to increase the electrical power generation while keeping greenhouse gas emissions minimized. This desire has led to the installation of renewable resources close to the load side instead of using the conventional power generators at the upstream of the power system[1], [2]. A conventional power grid has a unidirectional power flow, whereas the distributed generation units (DGs) enable bidirectional power flow, and, hence, the power grid becomes an active system. A classical power grid is constructed without the consideration of distributed generation at the load side. Subsequently, DGs cannot be directly inter-tied. Most of the installed DG units are based on renewable energy resources such as wind and solar that require a power electronic interfacing converter. The practical method of interfacing renewable sources into a classical power grid uses power electronic converters such as voltage source converters (VSCs). More importantly, VSCs can be used in high voltage applications such as HVDC[3] or medium voltage applications such as AC microgrids[4]. Due to the vibrant nature of renewable energy resources, the voltage and frequency dynamics are highly impacted once DG units are connected [5]–[7]. It is reported that a high penetration level of VSC units induces system instability issues due to the absence of inertia in the static power electronic converters [5]–[7].

In general, a synchronous machine supports the system frequency and maintain the voltage regulation due to the existence of the system inertia that provides extra power reserves for a short time. However, in the distribution systems, the renewable power generation is connected via a VSC. Therefore, the main disadvantage of using a VSC is the lack of inertia. The high penetration of distributed energy resources (DER) in the distribution system raises the issue of the reduced stability margin and affects the system dynamics [8]–[10]. Consequently, it is necessary to increase system stability especially with the high penetration level of DER units.

The virtual synchronous machine (VSM) control algorithm is recently introduced to remedy power system issues of low inertia [11]. The VSM control algorithm presents a new concept of a static power electronic inverter behaving as a synchronous machine (SM) [9]–[14]. This allows the interfacing inverter to have virtual inertia and provide damping to the system dynamics. In other words, a VSM can be defined as a combination of power electronic converter technology with SM characteristics. Because there is no physical mass of inertia in the VSC, it is merely a response of the converter power that mimics the inertia response of a real SM, depending on the energy stored in the existing dc-link capacitance. Several VSM control algorithms have been presented in the literature [12]–[14]. These types of VSM are sorted in terms of VSM output references [13], topologies [14], and controller order [12]. As demonstrated in [12], the VSM based on a second order swing equation is preferable, stable and reliable due to the use of classical cascaded current and voltage controller loops. However, designing the proper values of virtual inertia and damping, in order to achieve a stable and efficient performance, is still challenging [15].

The main contribution of this paper is to propose a new fully decoupled VSM control, based on the standard first order transfer function. To the author's best knowledge, this proposal, which is believed to extend the understanding in this trending field of research, has not been previously presented. The proposed controller provides an identical performance compared to the preferable and stable VSM model already proposed in literature [15], [16]. The test systems have been simulated in PSCAD/EMTDC environment.

This paper is organized into five sections: Section I outlines the determination behind introducing the VSM concept. Section II provides a brief description of VSMs based on the swing equation whereas Section III explains the proposed HVSM concept and its implementation. Section IV discusses simulation results and analysis, including the parameters of the system model used for the study. The final section presents the conclusions from this work

* **Corresponding Author**
Department of Electrical Engineering, Umm al-Qura University, Makkah, Saudi Arabia.
E-mail address: Hkrajhi@uqu.edu.sa (Hasan Alrajhi Alsiraji).

2. An Equivalence Conventional Frequency-Droop Control of the VSM

The VSM controller mainly uses the swing equation of traditional SMs in terms of active power based on Newton second law [13], [15]–[17], as shown in equation(1)

$$T_a.s.\omega_{vsm} = P_{mech} - P_{ele} - K_d(\omega_{vsm} - \omega_g) \quad (1)$$

where the mechanical time inertia is donated by T_a and the input power reference represents a mechanical power that is donated by P_{mech}. The electrical output converter power, based on the VSM, is represented by P_{ele}. The virtual damping coefficient of the converter is donated by K_d.The synchronous speed of the VSM is represented via the ω_{vsm} symbol. The last variable in the swing equation is ω_g, which determines the grid frequency using a phase locked loop (PLL).

The swing equation (1) can be rearranged, as shown in equation (2), which is identical to the conventional droop power equation as discussed in [13], [16]. Equation (3) presents the conventional droop power [16], [18], [19].

$$\frac{T_f.\omega}{m_p}.S = P_{mech} - P_{ele} - \frac{\omega - \omega_g}{m_p} \quad (2)$$

$$\omega = \omega_g - m_p(P_{mech} - P_{ele}) \quad (3)$$

The VSC, based on droop control without a low pass filter, (LPF) is inherently unstable [13], [18], and T_f is the time constant of the LPF. Hence, it is necessary to include a LPF in the power controller loop in order to stabilize the VSC and increase the quality of the power injection. As shown in equation (1), the virtual damping K_d is a reciprocal of the droop coefficient. Also, multiplying the reciprocal of the droop coefficient by the LPF time constant gives the virtual inertia T_a [13], [16].

$$T_a = {}^{T_f}/_{m_p}; \quad K_d = {}^{1}/_{m_p} \quad (4)$$

In fact, the main advantage of considering vector synchronous reference frame (SRF) control is to achieve decoupled independent control for active and reactive power. This control strategy is commonly used since it produces low voltage harmonics compared to direct power control [20]. However, the VSM concept re-links the active and reactive power due to the produced phase voltage angle θ_{vsm} via the swing equation [21]. The second order swing equation generates the voltage phase angle θ_{vsm} and the angular speed ω_{vsm} to energize the cascaded controller loops. Figure (1) shows a complete SRF block diagram of the VSM control concept applied to a VSC.

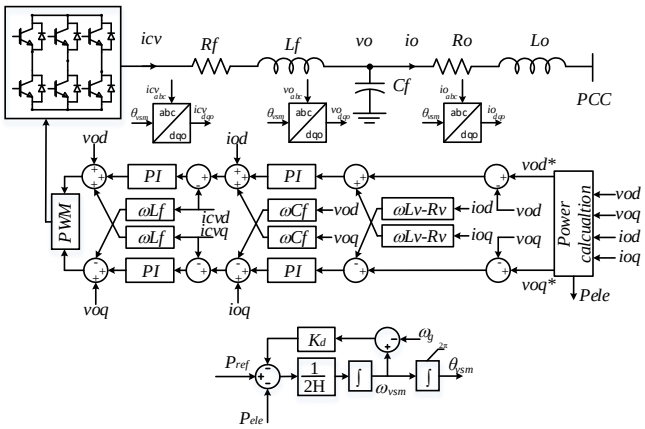

Figure 1: Complete Control Diagram of A VSC Converter Based on The Conventional VSM Controller.

3. The proposed hybrid VSM (HVSM)

As previously discussed, the VSM control concept introduces several advantages in terms of system frequency support, dynamic performance, and stability improvement. In this paper, a new straightforward HVSM is developed to mimic the SM behavior with better dynamics. The HVSM is achieved using a first order LPF for measuring the instantaneous fundamental powers instead of the first order LPF. The basic idea of the proposed HVSM offers a fully decoupled independent control for active and reactive power.

Since it is accepted that synchronous machines have inherent droop characteristics, it is preferable to write the swing equation as per unit, as shown in equation (5) [22]:

$$\frac{2H}{\omega_o}\frac{d^2\delta}{dt} = T_{mech} - T_{ele} - \frac{\mathrm{K_d}}{\omega_o}\frac{d\delta}{dt} \quad (5)$$

Based on the control theory, it is essential to present a system in the state space form to be expressed in a set of first order differential equations. Therefore, the swing equation can be split into two first order differential equations as follows:

$$\frac{d\Delta\omega_r}{dt} = \frac{1}{2H}\left(T_{mech} - T_{ele} - \mathrm{K_d}\frac{d\delta}{dt}\right) \quad (6)$$

$$\frac{d\delta}{dt} = \omega_o\Delta\omega_r \quad (7)$$

Further details are provided in [22], [23]. Referring to [24],equation (6) can be written in terms of active power by dividing both sides by angular frequency (ω) as illustrated in equation (8):

$$M\frac{d\omega^*}{dt} = P_{mech} - P_{ele} - D(\omega^* - \omega_o) \quad (8)$$

Manipulation by linearizing and arranging equation (8) through applying Laplace transformation represents the swing as shown in figure (2).

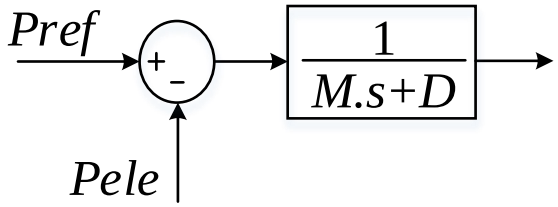

Figure 2: Swing Equation Representation into First Order Differential Equation

Based on figure (2), it is clear that using the conventional droop control means that the reference power command (P_{ref}) equals to zero. Therefore, considering a LPF to measure the fundamental active power lead the converter to mimic the governor and inertia behavior [18]. The absence of the LPF for measuring the fundamental active power in the a conventional droop control is interpreted as a converter with zero inertia; which means that the converter is inherently unstable [16]. As a result, including a first order LPF with convince parameter in the power feedback loop leads the converter based on active and reactive power control instead of AC voltage control to behave as a virtual synchronous machine (VSM). The control structure based on active and reactive power control is intensively used in HVDC system applications as well as the grid connected microgrids[25]–[27].

Generally, the operation of VSCs is inherently unstable without passing the measured power through first order LPF [15], [16], [18], [19]. On this basis, modifying the first order LPF coefficients gives some benefits listed as follow:

1. Completely fully decupled and independent control for the active and reactive power. To the author's best of knowledge, the proposed HVSM is the first controller offers independent active and reactive power control based on VSM concept due the fact that it does not require an external controller loop for the reactive to achieve a unity power factor.
2. The behavior of the VSC mimics the traditional SM since the droop control already exists in the first order filter. Furthermore, the proposed HVSM provides a better disturbance rejection.
3. The droop gain is embedded in the proposed HVSM design as illustrated in figure (2). Therefore, equal or different virtual damping coefficients (K_d) can be assigned to both active and reactive power controller.
4. The proposed HVSM can be easily applied by just modifying the LPF coefficients in order to achieve a traditional synchronous machine behavior.
5. In the connected mode of AC microgrid, all converters are working in the active and reactive power control mode[25], [28], as well as some of HVDC converter terminals[29]–[31]. Therefore, the proposed HVSM can be generically applied in different applications.

In equation (8), increasing the inertia constant (H) results in a slow VSC response, but provides better frequency regulation. Meanwhile, the value of damping ratio D is the main factor that stabilizes the VSC operation. The proposed HVSM implementation for the VSC controller is shown in figure (3).

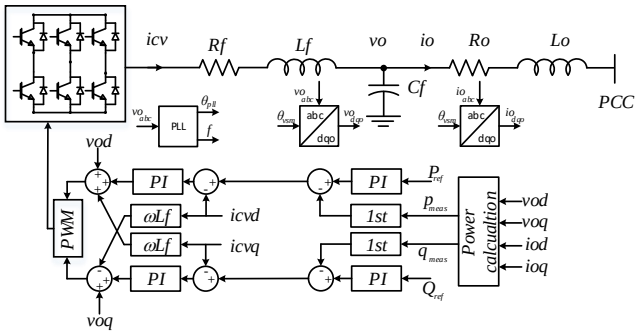

Figure 3: Schematic of the Proposed HVSM Controller.

4. Simulation results and analysis

The work presented in this paper involves an examination and comparison of the proposed HVSM with the VSM introduced in [16] that is comprehensively investigated and studied in [12]. The rationale for building both an HVSM and a VSM is the study and comparison of the static and dynamic properties. The system under study is presented in figure (4). The study is conducted using four different cases. These cases are based on an active power step change, system frequency drop, a three-phase short circuit that takes place at the AC side and, as in the last case, an AC voltage drop. The system parameters are set out in Table 1.

Table 1: VSC System Parameters

Quantity	Value	Unit
Converter rated power	100	MVA
AC Voltage (L-L) r.ms	24.5	kV
AC side resistance	0.025	Ω
AC side inductance	0.0048	H
System frequency	50	Hz
DC voltage	50	kV

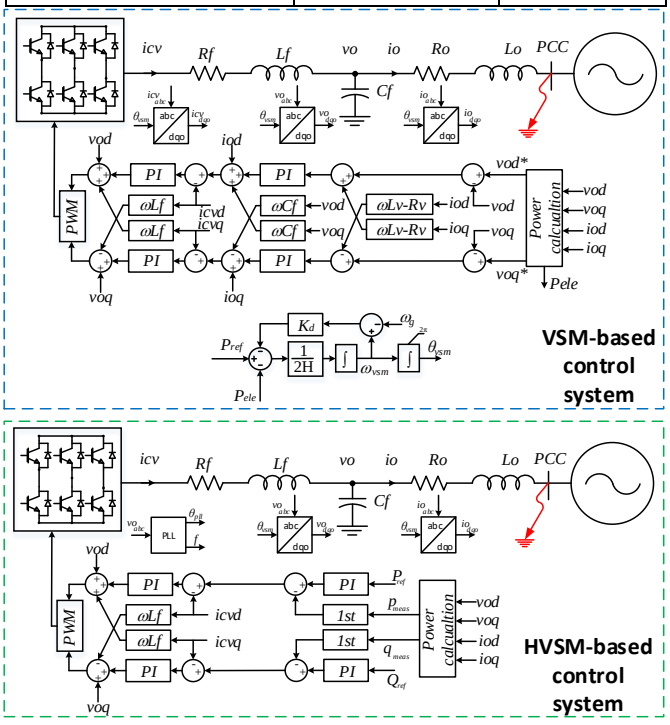

Figure 4: The System Under Study.

4.1. Case 1: Dynamic properties during load step changes for HVSM versus VSM

This first case demonstrates the performance of the proposed HVSM versus the VSM. Both VSCs as depicted in figure (4) are brought to the steady state, and the supplied power equals to zero, as shown in figure (5). At t = 1sec, the power reference for both VSCs increases from zero to 36MW. It can be clearly seen that both controllers have identical transient behavior. At t = 2sec, the load power references have further increased so that the VSCs supply the AC side by 80MW. The last step change for the power reference, which decreases from 80MW to 50MW, takes place at t =3sec. In this case, the proposed HVSM evidences a behavior similar to the VSM controller.

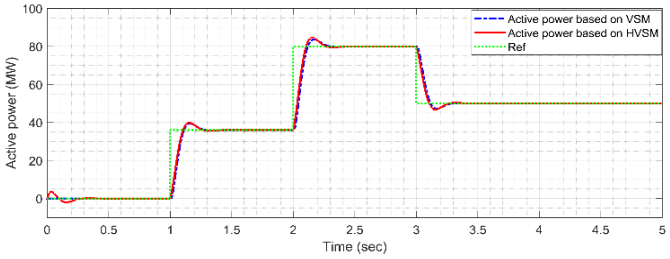

Figure 4: Active Power Response for Both Converters Based on VSM And HVSM During Step Power Change.

Due to the step load change at t = 1, 2, and 3sec, the system frequency responses for both systems are almost similar, as displayed in figure (6). It is observed that supplying a high level of power via both converters shows high transients in the system frequency, as shown in figure (6), at t = 2sec compared to the situation at t = 3sec. This phenomenon exists inherently in traditional SMs.

The reactive power based on HVSM is fully decoupled while the VSM is linked with the behavior of the active power reference. The main advantage of the proposed HVSM is that it can operate at unity power factor. The merits of the proposed HVSM over the VSM are clearly shown in figure (6).

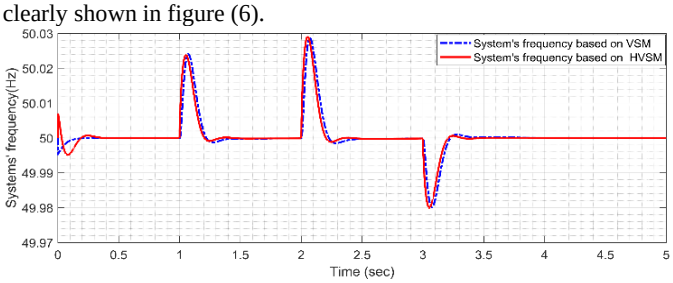

Figure 5: System Frequency Responses for Both Converters Based on VSM And HVSM During Step Power Change.

The behavior of the SM generator mainly depends on the load power factor changing. Therefore, supplying an inductive load via an SM generator significantly affects the phase voltage, hence operating the SM for the unity power factor – pure resistive load – leads to a slight decrease in the phase voltage, and vice versa for the capacitive load. This phenomenon based on SM voltage regulation characteristics is well-known and can be seen in figure (8). It is obvious that the proposed HVSM regulates the system voltage more effectively than the VSM because of the independent, active and reactive power control. This case proves that the HVSM emulates the behavior of a real synchronous generator. Even though the emulation of a virtual SM in terms of control of the VSC is achieved via both algorithms, the implementation of the HVSM-based model is simple and straightforward. Indeed, there is no doubt that both the proposed HVSM and the existing VSM offer identical response behavior with equal levels of accuracy.

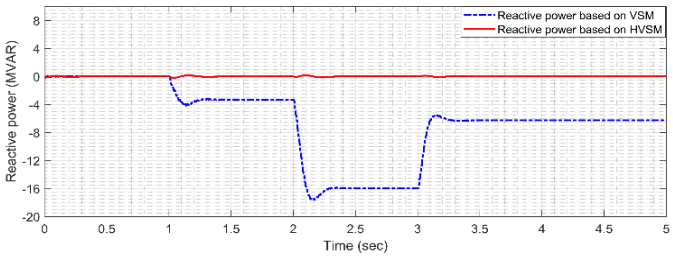

Figure 6: System Frequency Responses for Both Converters Based on VSM And HVSM During Step Power Change.

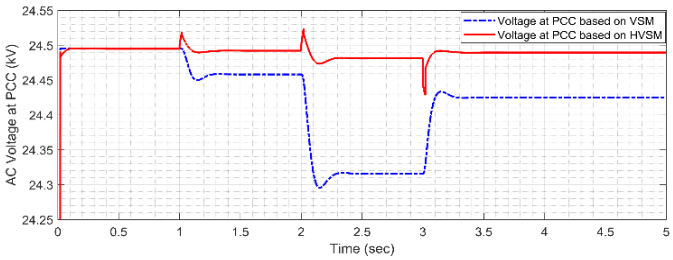

Figure 7: AC voltage response at PCC for both converters based on VSM and HVSM during step power change.

4.2. Case 2: Dynamic properties of HVSM versus VSM during system frequency drop:

The purpose of this case is only to evaluate the proposed HVSM over the existing VSM introduced in [16], [32]. In this case, the performance of the proposed HVSM versus the existing VSM is compared during system frequency variations. At t = 2sec, the system frequency is within an allowable range, which is a 0.2% decrease from 50Hz to 49.9Hz. Figure (9) shows that the performance for both VSMs during a system frequency drop is almost identical.

The system frequency is correlated to the active power injection. Thus, any change in the system frequency is reflected to the active power level, as known from the SM operation principle. Consequently, figure (10) reveals the effect of the system frequency drop on the active power. Based on the VSM controller at t = 2sec, the active power has a slight overshoot compared to the proposed HVSM. The rationale behind this difference is that the active and reactive powers are co-linked. Applying the direct-quadrature (d-q) SRF control theory with the VSM does not fully decouple the active and reactive powers due to the fact that the produced phase angle for the Park transformation block is produced by a swing equation [33].

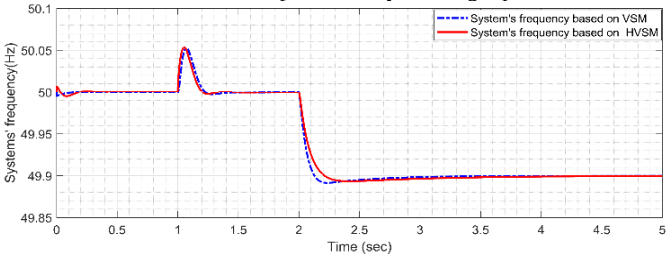

Figure 8: AC Voltage Response at PCC For Both Converters Based on VSM and HVSM During Step Power Change.

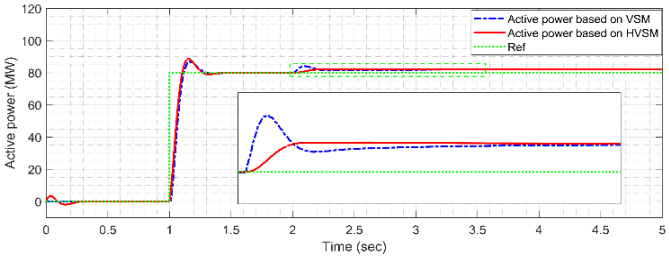

Figure 9: System Frequency Response for Both Converters Based on VSM And HVSM During Frequency Drop.

4.3. Case 3: Dynamic properties of HVSM versus VSM during system voltage drop

This third case shows the advantage of the proposed HVSM over the VSM. The proposed HVSM can offer a unity power factor feature, which is not present when applying the VSM. As can be seen in figure (11), the converters start supplying their AC side by 80MW at t = 1sec. At the same time, the converter based on VSM absorbs reactive power in order to meet the required active power, as displayed in figure (12). This phenomenon limits the total amount of active power transfer.

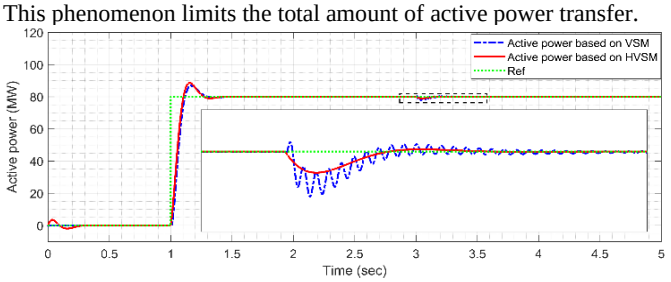

Figure 10: Active Power Response for Both Converters Based on VSM And HVSM During System Frequency Drop.

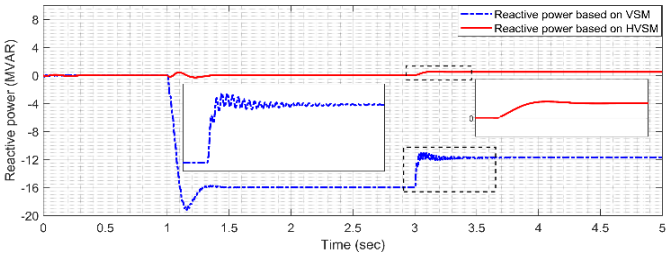

Figure 11: Reactive power response for both converters based on VSM and HVSM during step power change.

At t = 3sec, the system voltage drops from the nominal value (24.5kV) to 23.9kV, which is approximately equal to 0.975 p.u, as shown in figure (13). Hence, the VSM converter-based model decreases its reactive power consumption to compensate for the AC side voltage drop, as illustrated in figure (12). In contrast, the proposed HVSM meets the required active power command reference by supplying a considerably less amount of reactive power. The reason for this is that the droop characteristic is already embedded in the proposed HVSM, which can be designed separately from the active power based on operation requirements. However, at t = 3sec, the proposed HVSM tries to compensate for the AC side voltage drop by supplying a reactive power. The effect of the AC voltage drop on the active power can be observed in figure (11). In fact, the converter based on VSM raises an oscillatory occurrence on both active and reactive power transient responses. In contrast, the proposed HVSM provides well damped transient responses at t = 3sec, as can be seen in the zoomed sub-figures in figure (11), figure (13), respectively. The response of both the VSM and HVSM in emulating the SM is closely symmetrical. However, unlike the VSM, the proposed HVSM is capable of operating at a unity power factor. There is no doubt that the proposed HVSM offers more flexibility and freedom, especially for HVDC application.

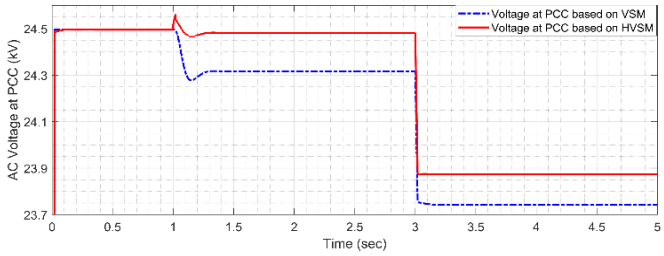

Figure 12: AC voltage response at PCC for both converters based on VSM and HVSM during step power change.

4.4. Case 4: Dynamic properties of HVSM versus VSM during a three-phase short circuit:

In this final case, both the VSM and the proposed HVSM are studied during three phases to ground fault. The fault takes place at the point of common coupling (PCC). The applied fault duration is five cycles (0.1sec) since most protection relays take action after five cycles. While both converters supply the AC load by 80MW, at t = 3sec the three phases to ground the short circuit are applied at PCC. The dynamic responses for both the active and frequency of each converter are shown in figure (14) and figure (15), respectively. From figure (14), it can be clearly realized that the converter based on the VSM has a higher active power transient response compared to the proposed HVSM. This is due to the fact that both active and reactive powers are linked by the swing equation. The active power during the fault of the converter based on VSM decreases 8% more than the converter based HVSM. In contrast, the system response based on the proposed HVSM gives a better and smaller overshoot response compared to the VSM.

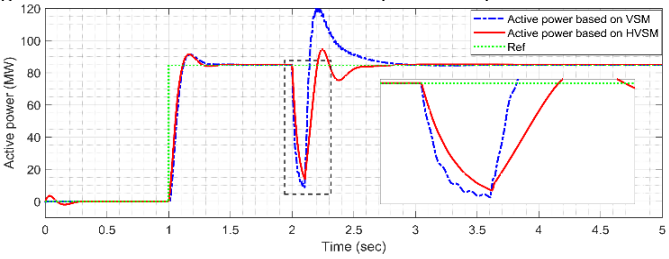

Figure 13: Reactive Power Response for Both Converters Based on VSM and HVSM During System Voltage Drop.

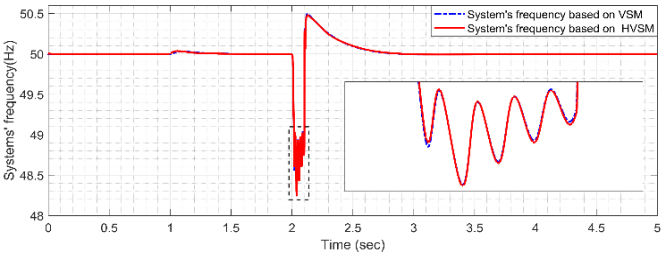

Figure 14: System Frequency Response for Both Converters Based on VSM and HVSM During a Three Phase Short Circuit.

Figure (15) presents the system frequencies for both converters, which are identical. The interpretation of the equivalence system frequencies is that both AC side converter frequencies are estimated using PLL. It is clear that, due to the short circuit, both the proposed HVSM and VSM frequencies are decreased and restored to the nominal operation value.

5. Conclusion

A new virtual synchronous machine control concept is proposed in this paper. A comprehensive comparison between the proposed HVSM and the existing VSM present in the literature has been conducted. Several advantages of the proposed HVSM are demonstrated. The proposed HVSM offers the substantial feature of a fully decoupled and independent control of the active and reactive power control. The implementation of the proposed HVSM in the VSC controller loops has also been illustrated. The significant outcomes of this paper are confirmed via time-domain simulations while the test system is simulated using a PSCAD/EMTDC environment.

6. Acknowledgments

The author acknowledges technical discussion with Dr. Mohammed Amin from the Norwegian University of Science and Technology.

7. References

[1] F. Iqbal, M. T. Khan, and A. S. Siddiqui, “Optimal placement of DG and DSTATCOM for loss reduction and voltage profile improvement,” *Alexandria Eng. J.*, vol. 57, no. 2, pp. 755–765, 2018.

[2] R. Majumder, A. Ghosh, G. Ledwich, and F. Zare, “Power sharing and stability enhancement of an autonomous microgrid with inertial and non-inertial DGs with DSTATCOM,” *2009 Int. Conf. Power Syst. ICPS ’09*, pp. 1–6, 2009.

[3] K. Alshammari, H. A. Alsiraji, and R. El Shatshat, “Optimal Power Flow in Multi-Terminal HVDC Systems,” in *2018 IEEE Electrical Power and Energy Conference, EPEC 2018*, 2018, pp. 1–6.

[4] H. Alrajhi Alsiraji and R. El-Shatshat, “Serious Operation Issues and Challenges Related to Multiple Interlinking Converters Interfacing a Hybrid AC/DC Microgrid,” in *Canadian Conference on Electrical and Computer Engineering*, 2018, pp. 1–5.

[5] V. Mendez, J. Rivier, and T. Gomez, “Assessment of Energy Distribution Losses for Increasing Penetration of Distributed Generation,” *IEEE Trans. Power Syst.*, vol. 21, no. 2, pp. 533–540, 2006.

[6] P. N. Vovos, A. E. Kiprakis, A. R. Wallace, and G. P. Harrison, “Centralized and distributed voltage control: Impact on distributed generation penetration,” *IEEE Trans. Power Syst.*, vol. 22, no. 1, pp. 476–483, 2007.

[7] A. K. Srivastava, A. A. Kumar, and N. N. Schulz, “Impact of distributed generations with energy storage devices on the electric grid,” *IEEE Syst. J.*, vol. 6, no. 1, pp. 110–117, 2012.

[8] Y. Chen, R. Hesse, D. Turschner, and H.-P. Beck, “Improving the grid power quality using virtual synchronous machines,” in *2011 International Conference on Power Engineering, Energy and Electrical Drives*, 2011, no. May, pp. 1–6.

[9] J. G. Slootweg and W. L. Kling, “Impacts of distributed generation on power system transient stability,” in *IEEE Power Engineering Society Summer Meeting*, 2002, vol. 2, pp. 862–867.

[10] Y. Chen, R. Hesse, D. Turschner, and H. Beck, “Comparison of methods for implementing virtual synchronous machine on inverters,” in *International Conference on Renewable Energies and Power Quality (ICREPQ’12)*, 2012, pp. 1–6.

[11] H.-P. Beck and R. Hesse, “Virtual synchronous machine,” in *2007 9th International Conference on Electrical Power Quality and Utilisation*, 2007, pp. 1–6.

[12] H. Alrajhi Alsiraji and R. El-Shatshat, “Comprehensive assessment of virtual synchronous machine based voltage source converter controllers,” *IET Gener. Transm. Distrib.*, vol. 11, no. 7, pp. 1762–1769, 2017.

[13] S. D. Arco and J. A. Suul, “Virtual Synchronous Machines – Classification of Implementations and Analysis of Equivalence to Droop Controllers for Microgrids,” in *PowerTech (POWERTECH), 2013 IEEE Grenoble*, 2013, pp. 1–7.

[14] H. Bevrani, T. Ise, and Y. Miura, “Virtual synchronous generators: A survey and new perspectives,” *Int. J. Electr. Power Energy Syst.*, vol. 54, pp. 244–254, Jan. 2014.

[15] S. D’Arco, J. A. Suul, and O. Fosso, “Automatic Tuning of Cascaded Controllers for Power Converters using Eigenvalue Parametric Sensitivities,” *IEEE Trans. Ind. Appl.*, vol. 9994, no. c, pp. 1–1, 2014.

[16] S. D’Arco and J. A. Suul, “Equivalence of Virtual Synchronous Machines and Frequency-Droops for Converter-Based MicroGrids,” *IEEE Trans. Smart Grid*, vol. 5, no. 1, pp. 394–395, 2014.

[17] S. D. Arco, J. A. Suul, and O. B. Fosso, “Small-Signal Modelling and Parametric Sensitivity of a Virtual Synchronous Machine,” in *Proceedings of the "18th Power Systems Computation Conference*, 2014, pp. 1–9.

[18] N. Pogaku, M. Prodanović, and T. C. Green, “Modeling, analysis and testing of autonomous operation of an inverter-based microgrid,” *IEEE Trans. Power Electron.*, vol. 22, no. 2, pp. 613–625, 2007.

[19] J. M. Guerrero, L. GarciadeVicuna, J. Matas, M. Castilla, and J. Miret, “A Wireless Controller to Enhance Dynamic Performance of Parallel Inverters in Distributed Generation Systems,” *IEEE Trans. Power Electron.*, vol. 19, no. 5, pp. 1205–1213, Sep. 2004.

[20] H. A. Alsiraji, “Operational Control and Analysis of a Hybrid AC / DC Microgrid,” University of Waterloo ,PhD thesis, 2018.

[21] H. Alrajhi Alsiraji, A. A. A. Radwan, and R. El-Shatshat, “Modelling and analysis of a synchronous machine-emulated active intertying converter in hybrid AC/DC microgrids,” *IET Gener. Transm. Distrib.*, vol. 12, no. 11, pp. 2539–2548, 2018.

[22] P. Kundur, *Power System Stability And Control*. McGraw-Hil, 1993.

[23] P. W. Sauer and M. Pai, *Power system dynamics and stability*. Pearson Education (US), 1997.

[24] M. Guan, W. Pan, J. Zhang, Q. Hao, J. Cheng, and X. Zheng, “Synchronous Generator Emulation Control Strategy for Voltage Source Converter (VSC) Stations,” *IEEE Trans. POWER Syst.*, vol. 30, no. 6, pp. 1–9, 2015.

[25] A. J. Agbemuko, J. L. Domínguez-García, E. Prieto-Araujo, and O. Gomis-Bellmunt, “Dynamic modelling and interaction analysis of multi-terminal VSC-HVDC grids through an impedance-based approach,” *Int. J. Electr. Power Energy Syst.*, vol. 113, no. January, pp. 874–887, 2019.

[26] R. Joan, L. Alvaro, B. Frede, and R. Pedro, “Control of Power Converters in AC Microgrids,” *IEEE Trans. POWER Electron.*, vol. 27, no. 11, pp. 4734–4749, 2012.

[27] H. A. Alsiraji, “Cooperative Power Sharing control in Multi-terminal VSC-HVDC,” 2014.

[28] Y. Gui, X. Wang, F. Blaabjerg, and D. Pan, “Control of Grid-Connected Voltage-Source Converters: The Relationship Between Direct-Power Control and Vector-Current Control,” *IEEE Ind. Electron. Mag.*, vol. 13, no. 2, pp. 31–40, 2019.

[29] T. H. Nguyen, K. Hassan Al Hosani, and M. El Moursi, “Alternating Submodule Configuration Based MMCs with Carrier-Phase-Shift Modulation in HVDC Systems for DC-Fault Ride-Through Capability,” *IEEE Trans. Ind. Informatics*, vol. 3203, no. c, pp. 1–1, 2019.

[30] T. H. Nguyen, K. Al Hosani, M. S. El Moursi, and N. Al Sayari, “A Submodule-Capacitor Voltage Balancing Strategy for Alternative-Arm Converters in HVDC Systems,” *IEEE Trans. Power Deliv.*, vol. 34, no. 3, pp. 795–806, 2019.

[31] M. A. A. Murad and F. Milano, “Modelling and Simulation of PI-controllers Limiters for the Dynamic Analysis of VSC-based Devices,” *IEEE Trans. Power Syst.*, vol. 8950, no. c, pp. 1–1, 2019.

[32] S. D’Arco, J. A. Suul, and O. B. Fosso, “Small-signal modeling and parametric sensitivity of a virtual synchronous machine in islanded operation,” *Electr. Power Energy Syst.*, vol. 72, pp. 3–15, 2015.

[33] Q. C. Zhong and G. Weiss, “Synchronverters: Inverters that mimic synchronous generators,” *IEEE Trans. Ind. Electron.*, vol. 58, no. 4, pp. 1259–1267, 2011.